

Supporting information for

# Theoretical Insights into the Interactions between Star-shaped Antimicrobial Polypeptides and Bacterial Membrane

*Yunhan Zhang<sup>†</sup>, Tongwei Chen<sup>†</sup>, Zhimeng Pan<sup>‡</sup>, Xianbao Sun<sup>†</sup>, Xue Yin<sup>†</sup>, Miao He<sup>†</sup>, Shiyan Xiao<sup>†,\*</sup>, Haojun Liang<sup>†,¶</sup>*

<sup>†</sup> CAS Key Laboratory of Soft Matter Chemistry, iChEM (Collaborative Innovation Center of Chemistry for Energy Materials), Department of Polymer Science and Engineering, University of Science and Technology of China, Hefei, Anhui 230026, P. R. China.

<sup>‡</sup> School of Computing, University of Utah, Salt Lake City, UT 84112, United States of America

<sup>¶</sup> Hefei National Laboratory for Physical Sciences at the Microscale, University of Science and Technology of China, Hefei, Anhui 230026, P. R. China.

\*To whom correspondence should be addressed. E-mail: [xiaosy@ustc.edu.cn](mailto:xiaosy@ustc.edu.cn) (S. X.)

## Supporting figures.

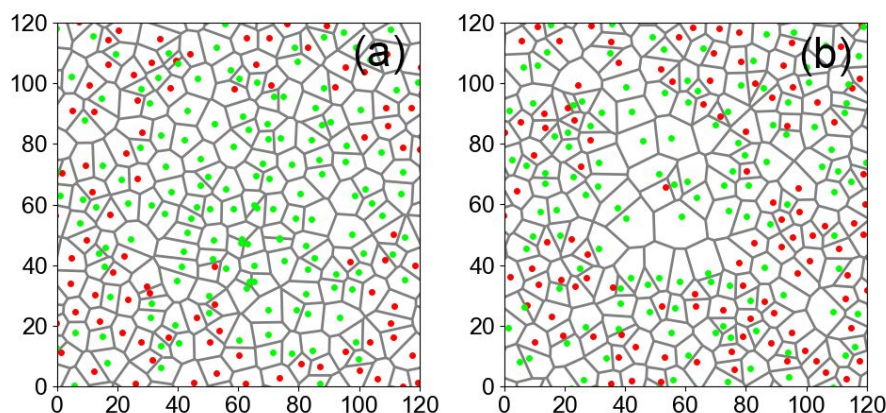


**Figure S1** Area per bead for head beads of POPE (red) and POPG (green). The membrane bilayer consists of 640 POPE and 640 POPG with its ratio equals 1:1. The two panels represent the membrane interacting with star-KV ( $D_c=1.5\text{nm}$ ,  $N_g=25$ ) (a), star-CM15 ( $D_c=1.5\text{nm}$ ,  $N_g=25$ ) (b), displayed within the range of (0, 12)nm for  $X$  axis and the range of (0, 12)nm for  $Y$  axis, respectively.

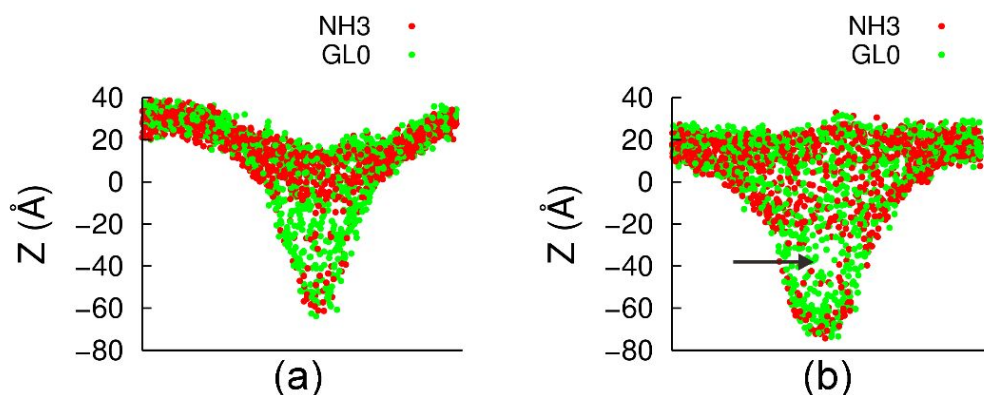


**Figure S2** Side view of the membrane when interacts with star-KV ( $D_c=5\text{nm}$ ,  $N_g=70$ ) (a) and star-CM15 ( $D_c=5\text{nm}$ ,  $N_g=70$ ) (b) by using scatter points. The membrane consists of 2000 POPE and 2000 POPG, with a ratio of 1:1, red point represents the head bead of POPE, green point represents the head bead of POPG, the arrow mark the membrane defects.

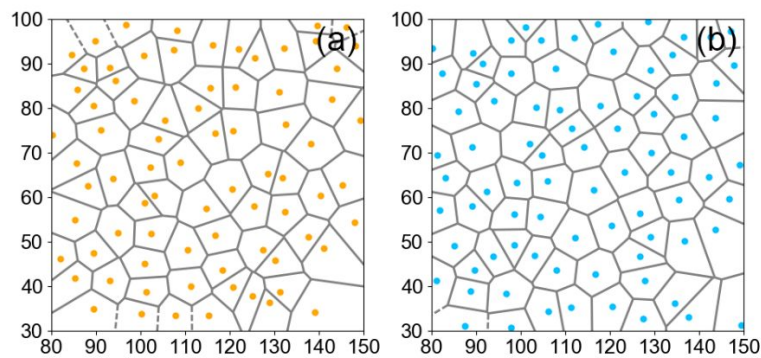


**Figure S3** Area per bead for positive head beads (orange point) and negative head beads (blue point) of 1270 DPPC interacting with absent particle, (a) and (b) displayed within the range of (8, 15) nm for X axis and the range of (3,10) nm for Y axis respectively.

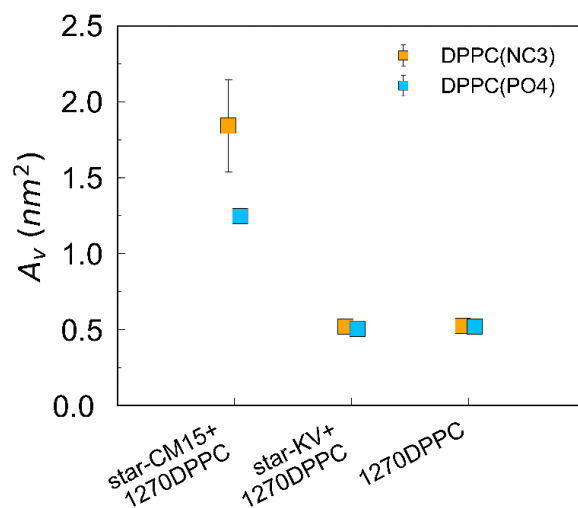


**Figure S4** Area per bead,  $A_v$ , for positive head bead (orange) and negative head bead (blue) of 1270 DPPC interacting with star-CM15, star-KV and absence of star-AMP after 1 us.

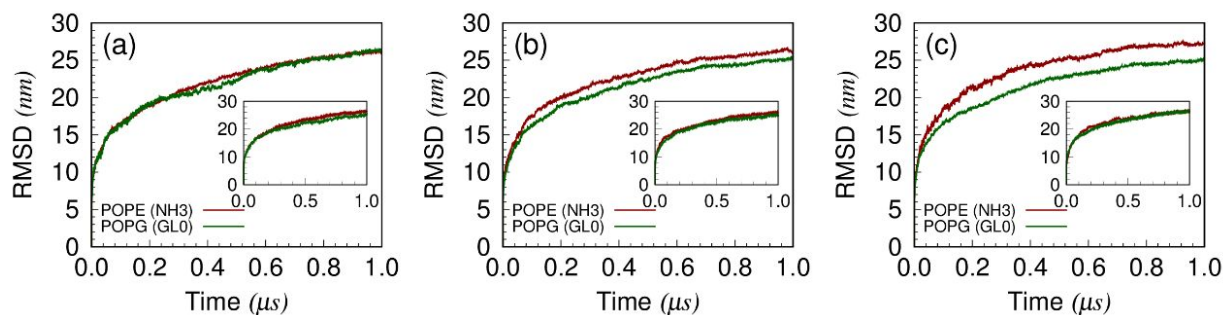


**Figure S5** The root mean square deviation (RMSD) for head bead “NH3” of POPE lipid (darkred curve) and “GL0” of POPG lipid (darkgreen curve) as a function of time (in  $\mu\text{s}$ ). Star-KV ( $D_c=1.5\text{nm}$ ,  $N_g=25$ ) interact with the mixed POPE and POPG lipid bilayer with various ratios, that is, (a) 7200 POPE: 1800 POPG (4:1); (b) 4500 POPE: 4500 POPG (1:1); (c) 1800 POPE: 7200 POPG (1:4). The inset of each panel corresponds to RMSD of a system with the same membrane with small star-CM15 ( $D_c=1.5\text{nm}$ ,  $N_g=25$ ).

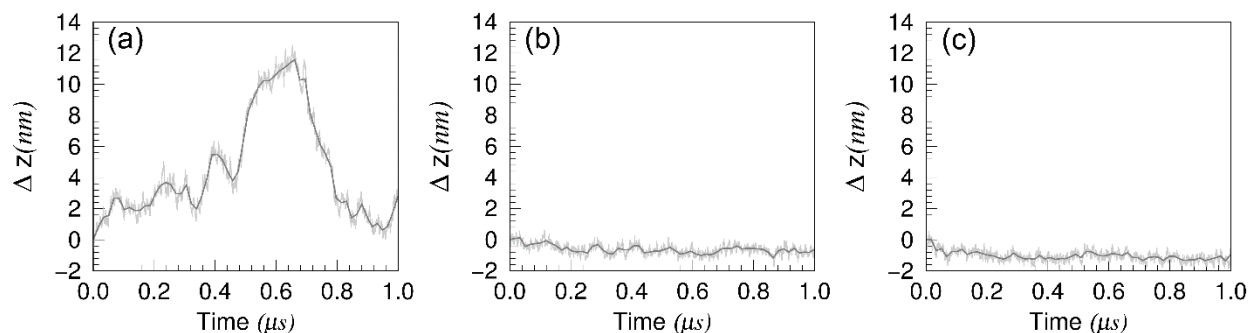


**Figure S6** Time evolution of the change in the distance between the center of mass of the star-AMP and the DPPC bilayer ( $\Delta z$ ) are shown as the evolution time of interaction for both star- $(K_2V_1)_5 + 5e$  (a), star-KKV( $K_2F_1$ ) $_4 + 10e$  (b) and star-KKV(KLF) $_4 + 6e$  (c).

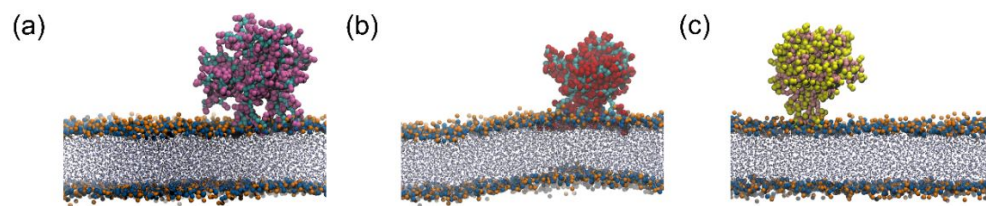


**Figure S7** The star-shaped nanoparticles have coil configuration grafts. Side view snapshots of the interactions of star-KKV( $K_2F_1$ )<sub>4</sub> (a), star-KKV(KLF)<sub>4</sub> (b) and star-CM15 with a 1270DPPC bilayer after 1 $\mu$ s MD simulations.

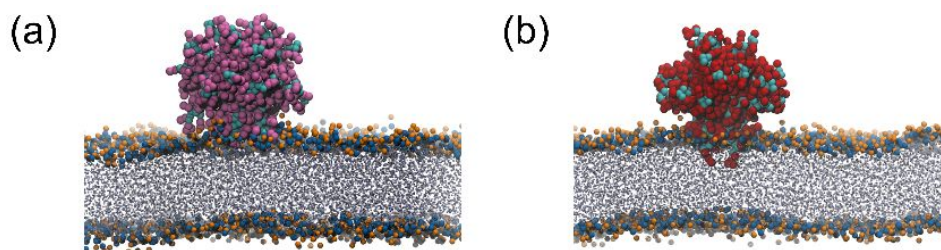


**Figure S8** The star-shaped nanoparticles have  $\alpha$ -helix configuration grafts. Side view snapshots of the interactions of star-KKV( $K_2F_1$ )<sub>4</sub> (a), star-KKV(KLF)<sub>4</sub> (b) with a 1270DPPC bilayer after 1 $\mu$ s MD simulations.

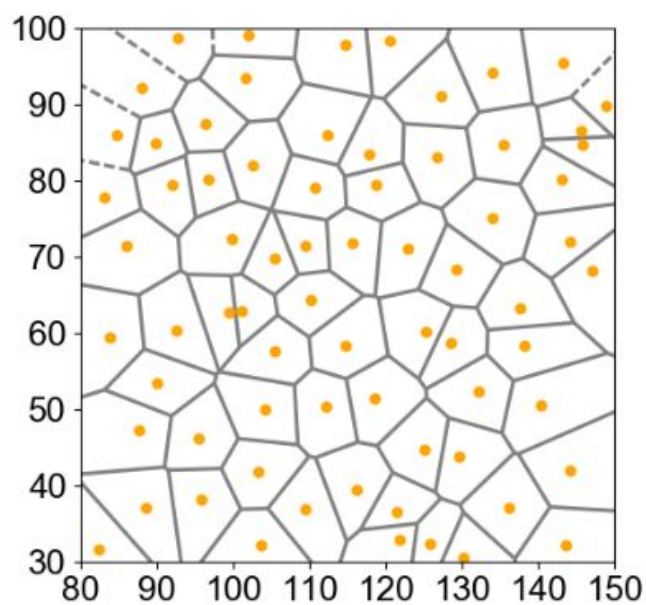


**Figure S9** Area per bead for positive head beads (orange point) of DPPC and DLiPC with the absence of polypeptide, displayed within the range of (8, 15) nm for X axis and the range of (3,10) nm for Y axis respectively.

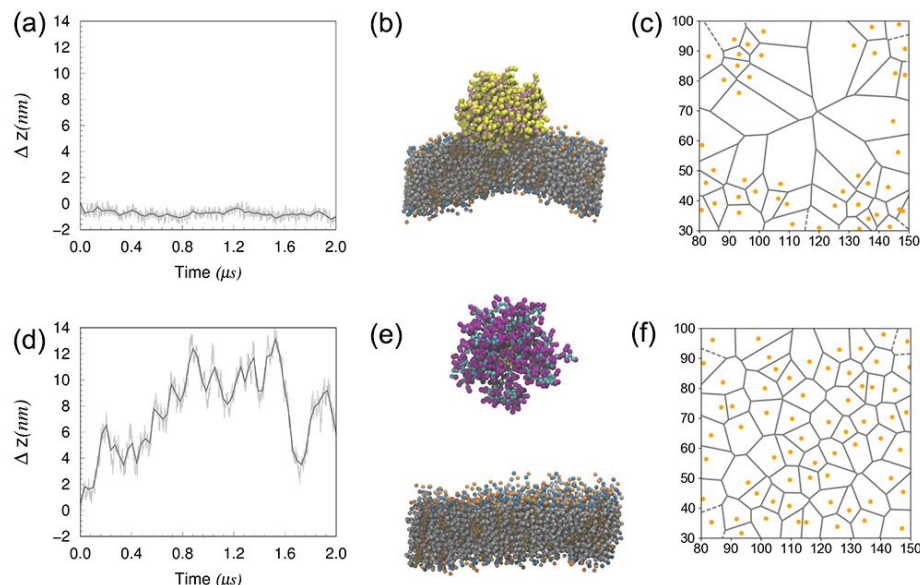


**Figure S10** Time evolution of the change in the distance of the centers of mass between star-AMP and the complexity of 769DPPC:507DLiPC:538 cholesterol bilayer ( $\Delta z$ ) for star-CM15 (a) and star-KV (d), with their equilibrium states shown in the (b) and (e) respectively, DPPC and DLiPC lipids different with each other in hydrocarbon tails (silver) and have the same kind of beads, that is, NC3 (orange) and PO4 (blue). The cholesterol shows in brown. The area of each bead is determined for the positive head NC3 (orange point) of DPPC and DLiPC lipids, using the Voronoi tessellation of the coordinates of the head beads. Displayed range: (8, 15) nm for X axis, (3, 10) nm for Y axis. The systems are constructed using 1270 DPPC molecules being integrated with one star-CM15 (c) or one star-KV (f).



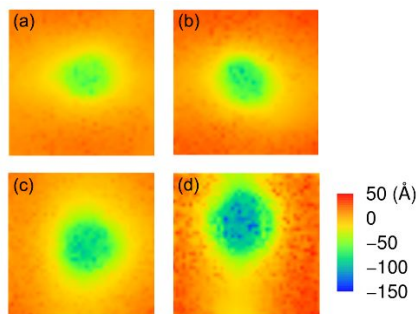


**Figure S11** Deviation of lipid at z direction for the PE/PG bilayer interacting with star-CM15 ( $D_c = 5$  nm,  $N_g = 70$ ) (a), star-KV ( $D_c = 5$  nm,  $N_g = 70$ ) (b), and star-CM15 ( $D_c = 5$  nm,  $N_g = 150$ ) (c), star-KV ( $D_c = 5$  nm,  $N_g = 150$ ) (d). Note that the lipid composition of the bilayer is 1:4 (800 POPE : 3200 POPG).

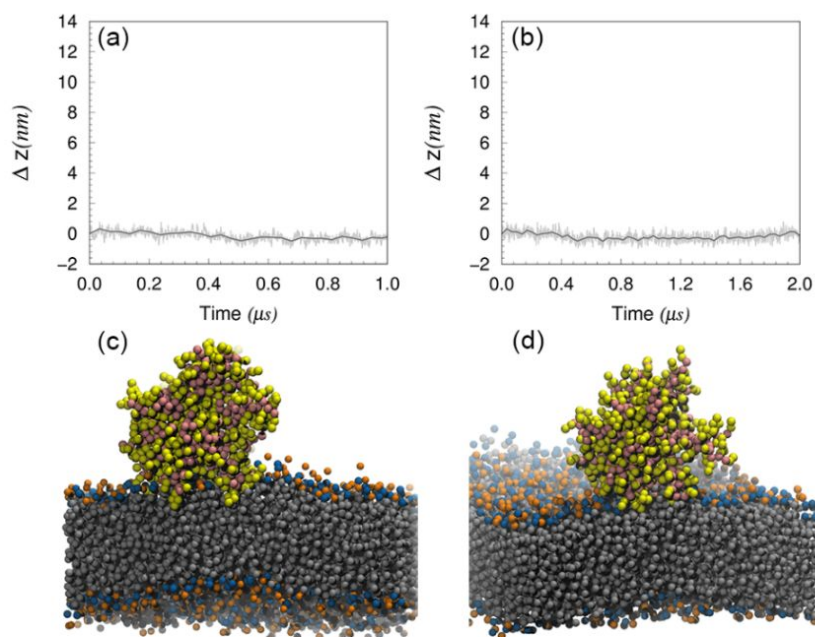


**Figure S12** Time evolution of the change in the distance of the centers of mass between star-CM15 and DPPC bilayer ( $\Delta z$ ) for 1.0  $\mu s$  (a) and 2.0  $\mu s$  MD simulation (b), with their equilibrium states of VMD snapshots shown in the (c) and (d). Each bead is determined for the positive head NC3 (orange point), the negative head PO4 (blue point) and the hydrocarbon tails beads (silver point). The systems are constructed using the bilayer formed using 1270 DPPC molecules being integrated with one star-CM15.



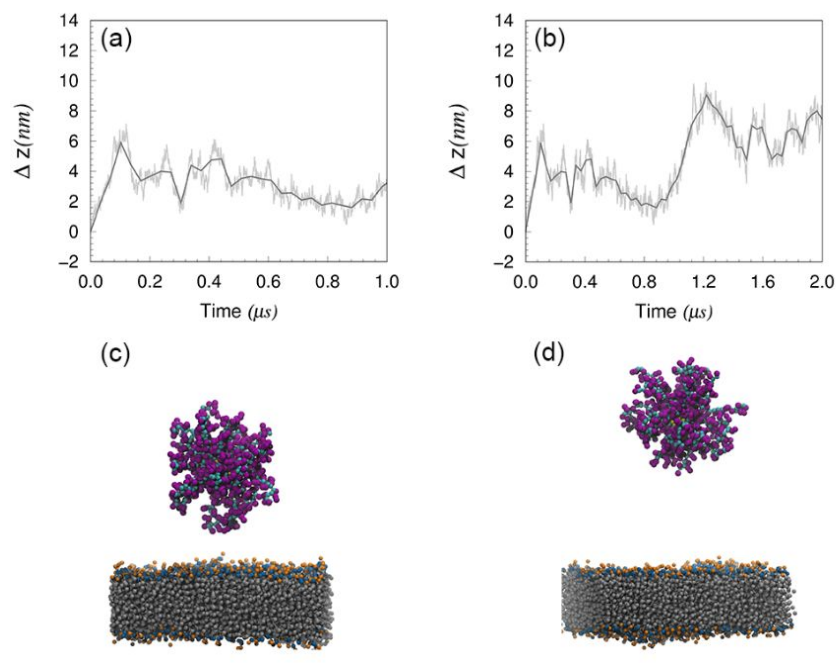


**Figure S13** Time evolution of the change in the distance of the centers of mass between star-KV and DPPC bilayer ( $\Delta z$ ) for 1  $\mu s$  (a) and 2  $\mu s$  MD simulation (b), with their equilibrium states of VMD snapshots shown in the (c) and (d). Each bead is determined for the positive head NC3 (orange point), the negative head PO4 (blue point) and the hydrocarbon tails beads (silver point). The systems are constructed using 1270 DPPC molecules being integrated with one star-KV.

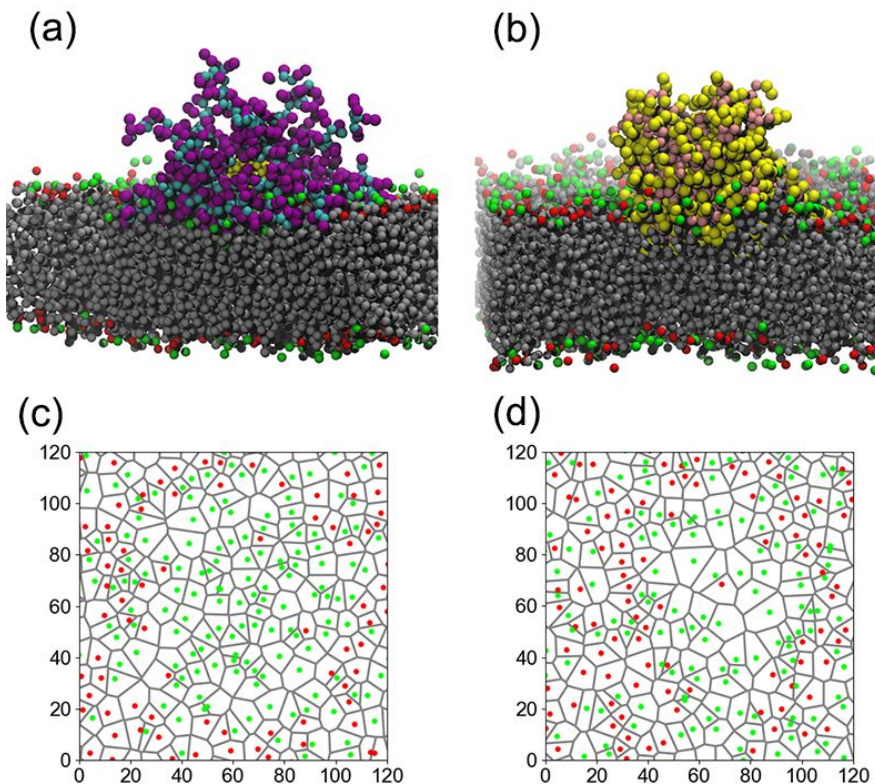


**Figure S14** Side view snapshots of the interactions of star-KV (a) and star-CM15 (b), with a 640 POPE: 640 POPG bilayer after 2 $\mu$ s MD simulations. For clarity, the core of the star-shaped polypeptide is depicted in light-orange, the main and side chains of (K<sub>2</sub>V<sub>1</sub>)<sub>5</sub> are in cyan and purple, respectively; and that of CM15 are in pink and yellow, respectively. The bead of the positively charged head NH<sub>3</sub> of POPE is in red, the bead of the negatively charged head GL0 of POPG is in green, and the hydrocarbon tails is silver. Area per bead for head beads of POPE (red) and POPG (green). The membrane bilayer consists of 640 POPE and 640 POPG with its ratio equals 1:1. The two panels represent the membrane interacting with star-KV ( $D_c=1.5\text{nm}$ ,  $N_g=25$ ) (c), star-CM15 ( $D_c=1.5\text{nm}$ ,  $N_g=25$ ) (d) after 2 $\mu$ s MD simulations, displayed within the range of (0, 12)nm for X axis and the range of (0, 12)nm for Y axis, respectively.

**Table S1** The information of the systems.

system	box size (nm)	number (total)	number (water)	number (ions)
1star-KV+640POPE:640POPG ( $D_c = 1.5nm, N_g = 25$ )	20.0x20.0x20.0	65568	48683	390 NA+
1star-CM15+640POPE:640POPG ( $D_c = 1.5nm, N_g = 25$ )	20.0x20.0x20.0	65501	48591	515 NA+
1star-KV+800POPE:3200POPG ( $D_c = 5nm, N_g = 70$ )	35.6x35.6x30.0	315126	260806	2500 NA+
1star-CM15+800POPE:3200POPG ( $D_c = 5nm, N_g = 70$ )	35.6x35.6x30.0	315811	261421	2850 NA+
1star-KV+2000POPE:2000POPG ( $D_c = 5nm, N_g = 70$ )	35.3x35.3x25.0	255408	202288	1300 NA+
1star-CM15+2000POPE:2000POPG ( $D_c = 5nm, N_g = 70$ )	35.3x35.3x23.0	237495	184305	1650 NA+
1star-KV+3200POPE:800POPG ( $D_c = 5nm, N_g = 70$ )	35.1x35.1x25.0	253736	201816	100 NA+
1star-CM15+3200POPE:800POPG ( $D_c = 5nm, N_g = 70$ )	35.1x35.1x23.0	236017	184027	450 NA+
25star-KV+1800POPE:7200POPG ( $D_c = 1.5nm, N_g = 25$ )	53.5x53.5x30.0	712587	575262	950 NA+
25star-CM15+1800POPE:7200POPG ( $D_c = 1.5nm, N_g = 25$ )	53.5x53.5x29.0	682541	544591	4075NA+
25star-KV+4500POPE:4500POPG ( $D_c = 1.5nm, N_g = 25$ )	53.1x53.1x29.0	673806	534282	1750 CL-
25star-CM15+4500POPE:4500POPG ( $D_c = 1.5nm, N_g = 25$ )	53.1x53.1x29.0	676942	541692	1375 NA+

25star-KV+7200POPE:1800POPG ( $D_c = 1.5nm, N_g = 25$ )	52.7x52.7x30.0	700833	560008	4450 CL-
25star-CM15+7200POPE:1800POPG ( $D_c = 1.5nm, N_g = 25$ )	52.7x52.7x29.0	671065	535865	1325 CL-
1star-KV+1270DPPC ( $D_c = 1.5nm, N_g = 25$ )	19.7x19.7x26.5	87927	72327	250 CL-
1star-CM15+1270DPPC ( $D_c = 1.5nm, N_g = 25$ )	19.7x19.7x19.7	63928	47528	125 CL-
1star-KV+769DPPC+507DLiPC+538cholesterol ( $D_c = 1.5nm, N_g = 25$ )	21.8x21.8x28.0	112289	91288	250 CL-
1star-CM15+769DPPC+507DLiPC+538cholesterol ( $D_c = 1.5nm, N_g = 25$ )	21.8x21.8x19.0	78243	57464	125 CL-
1star-KV+800POPE:3200POPG ( $D_c = 5nm, N_g = 150$ )	35.6x35.6x32.0	331765	274885	1700 NA+
1star-CM15+800POPE:3200POPG ( $D_c = 5nm, N_g = 150$ )	35.6x35.6x32.0	332689	275659	2450 NA+

## Supporting text

To examine whether the simulation time used in the present work (*i.e.*, 1.0  $\mu\text{s}$ ) is long enough or not for the simulated systems to achieve their equilibrium for analyzing, four representative systems were taken as examples to examine the equilibrium by extending the simulation time from 1.0  $\mu\text{s}$  to 2.0  $\mu\text{s}$ . The four systems are listed as following.

- i) the star-CM15 ( $D_c=1.5\text{nm}$ ,  $N_g=25$ ) + 1270 DPPC bilayer membrane;
- ii) the star-CM15 ( $D_c=1.5\text{nm}$ ,  $N_g=25$ ) + mixed 640POPE and 640POPG bilayer membrane;
- iii) the star-KV ( $D_c=1.5\text{nm}$ ,  $N_g=25$ ) + 1270 DPPC bilayer membrane;
- iv) the star-KV ( $D_c=1.5\text{nm}$ ,  $N_g=25$ ) + mixed 640POPE and 640POPG bilayer membrane;

First, we studied the time evolution of the change in the distance of the centers of mass between star-CM15 and DPPC bilayer ( $\Delta z$ ). As shown in Figure S12a and S12b, star-CM15 remained a tight contact with the DPPC bilayer membrane after its landing onto bilayer, and no detachment has been observed as we extended the MD simulation from 1.0  $\mu\text{s}$  to 2.0  $\mu\text{s}$ . We further checked the configuration of star-CM15 (Figure S12c and S12d), and found that there is no significant change for the star-CM15 at 1.0  $\mu\text{s}$  and 2.0  $\mu\text{s}$ . For star-KV, it “floated” in the aqueous space above the DPPC bilayer, and no contact was observed in the whole simulation trajectory (Figure S13a and S13c). The extended trajectory of 2.0  $\mu\text{s}$  for the star-KV interacting with DPPC bilayer confirmed the validity of our above observation (Figure S13b and S13d).

Then, we studied the interactions between star-CM15 and star-KV with the mixed 640POPE and 640POPG bilayer membrane. The side view snapshots of the star-AMP and bilayer system at 1.0  $\mu\text{s}$  are shown in Figure 2 of the main text, and the area per bead for head beads of POPE and POPG of the membrane is shown in Figure S1 of the Supporting Information. The results derived from the extended trajectories of 2.0  $\mu\text{s}$  are depicted in Figure S14.

From the 1.0  $\mu\text{s}$  trajectories, we found that both the star-CM15 and star-KV landed onto the bilayer quickly. After landing onto the membrane, the hydrophobic residues of CM15 near the membrane tended to interact with the hydrophobic tails of lipids, insert the grafts into the interior of membrane. Star-CM15 shrank its size because of the hydrophobic effects, whereas, the star-KV resulted in a divergent star-shaped configuration because of the much larger amount of positive charge than that of star-CM15. The flattened configuration of star-KV occupied a larger area on the membrane than the star-CM15, and therefore presented a larger domain constituted by “frozen”

PG lipids (Figure 3a,b, and Figure S1). As we extended the MD simulations from 1.0  $\mu$ s to 2.0  $\mu$ s, the same results were derived, and the above conclusions were fully supported (Figure S14).

## Supporting video.

Nine videos were enclosed to present the evaluated streamline patterns of lipid movements for the upper leaflet of the membrane. The star-AMPs ( $D_c = 1.5\text{nm}$ ,  $N_g = 25$ ) NPs were depicted in purple.

The **Video S1** and **Video S2** shows the streamline patterns of the star-KV and the star-CM15 interacting with the mixed POPE and POPG bilayer with a ratio of 4:1 (7200 PE, 1800 PG), respectively. The **Video S3** is the pure membrane with a ratio of 4:1 (7200 PE, 1800 PG).

The **Video S4** or **Video S5** shows the streamline patterns of star-KV or star-CM15 interacting with the mixed POPE and POPG bilayer with a ratio of 1:1 (4500 PE, 4500 PG), respectively. The **Video S6** is the pure membrane with a ratio of 1:1 (4500 PE, 4500 PG).

The **Video S7** or **Video S8** shows the streamline patterns of star-KV or star-CM15 interacting with the mixed POPE and POPG bilayer with a ratio of 1:4 (1800 PE, 7200 PG), respectively. The **Video S9** is the pure membrane with a ratio of 1:4 (1800 PE, 7200 PG).